Biosensors and Bioelectronics 26 (2011) 3413–3419

Contents lists available at ScienceDirect

Biosensors and Bioelectronics

journal homepage: www.elsevier.com/locate/bios

Development of a microfluidic cell-based biosensor integrating a millisecond chemical pulse generator

Jian Sun [1], Pu Chen [1], Xiaojun Feng, Wei Du, Bi-Feng Liu *

Britton Chance Center for Biomedical Photonics at Wuhan National Laboratory for Optoelectronics–Hubei Bioinformatics & Molecular Imaging Key Laboratory, Department of Systems Biology, College of Life Science and Technology, Huazhong University of Science and Technology, Wuhan 430074, China

ARTICLE INFO

Article history:
Received 9 December 2010
Accepted 10 January 2011
Available online 19 January 2011

Keywords:
Cell-based biosensor
Microfluidic chip
Hydrodynamic gating
ATP
Calcium imaging

ABSTRACT

The use of cell-based biosensors is usually limited by agonist-induced desensitization of cell-surface receptors. In this work, a microfluidic cell-based biosensor (μCBB) was developed for the detection of ATP in liquid environments. It consists of a millisecond chemical pulse generator for sample introduction in a pulsatile manner and a single NIH-3T3 cell expressing endogenous P2Y receptors as the sensing element. ATP solutions were used to simulate input signals for investigating the μCBB. By controlling negative pressures on two outlets of a cross-shaped microfluidic chip, pulses of ATP solutions were generated based on hydrodynamic gated injection. With ATP pulses of 100 ms every 50 s, the amplitude of the resulting calcium spikes maintained at a similar level, suggesting that the receptor desensitization was minimized. Consequently, the developed μCBB could be used for detecting pulsatile samples with extended use times. The sensitivity of the μCBB for detecting ATP was further determined and the cellular responses to millisecond ATP pulses were investigated in comparison to long-term stimulations.

1. Introduction

Humans or other living animals are influenced by substances in their environment such as drugs, pathogens and toxicants. It is sometimes necessary to monitor the existence of such "environment threats" for safety precautions. Biosensors are miniaturized devices that are capable of defecting biorelevant substances with high sensitivity and specificity. For example, glucose sensors have been widely employed as point-of-care testing devices for determining the glucose level in patients suffering from diabetes (Hu, 2009).

Biosensors usually consist of a sensing element for the recognition of target molecules and a transducer for signal transduction. The sensing element is the key component of a biosensor. The emerging cell-based biosensors (CBBs) utilize living cells as the sensing elements. The main advantages of cells as sensing elements come from their built-in naturally occurring chemical receptors that are responsive to specific target molecules. Activation of these receptors elicits a number of cellular responses that can be monitored optically or electrochemically, including changes in intracellular calcium ion concentration ($[Ca^{2+}]_i$), transmembrane potential and metabolic activity (Zhang et al., 2006; Sigworth and Klemic, 2002; Klemic et al., 2002). By monitoring these receptor-mediated cellular responses, it is possible to determine minute amounts of target molecules in liquid environments with high specificity.

Currently, CBBs have shown potentials for a variety of sensing applications (Hazama et al., 1998; Gray et al., 2001; Matsubara et al., 2004; Xu et al., 2005; Curtis et al., 2008; Suska et al., 2009). The functionality of CBBs depends on the receptor-mediated cellular responses. Existing receptors can be generally categorized into two classes, i.e., ligand-gated ion channels and G-protein coupled receptors (GPCRs) (Boehm and Kubista, 2002). Both types of receptors have been successfully implemented in CBBs. Hayashi et al. reported the use of P2X receptors, a type of ligand-gated ion channel for detecting ATP in solutions by monitoring the receptor-mediated Ca^{2+} influx with patch clamp techniques (Hayashi et al., 2004). Recently, Feng et al. explored the feasibility of using a bullfrog fibroblast cell line (FT cells) expressing P2Y receptors, a type of GPCRs as the basis of a cell-based biosensor (Feng et al., 2007). Using this device, they were able to detect ATP in solutions by monitoring rises in intracellular calcium optically or the secretion of pre-loaded norepinephrine electrochemically.

Receptor-mediated cellular responses have proven to be a reliable basis for CBBs (Aravanis et al., 2001; Lee et al., 2009). However, there are limitations regarding the use of receptors due to the desensitization of receptors upon long-term stimulations, which results in loss of cellular responses (Banerjee and Bhunia, 2009; Fishman et al., 1998). To overcome this issue, one strategy was proposed previously by Fishman et al., in which single-cell arrays were developed for multiple detections (Fishman et al., 1996). Since the

* Corresponding author. Tel.: +86 27 87792203; fax: +86 27 87792170.
E-mail address: bfliu@mail.hust.edu.cn (B.-F. Liu).
[1] These authors contributed equally to this work.

0956-5663/$ – see front matter © 2011 Elsevier B.V. All rights reserved.
doi:10.1016/j.bios.2011.01.013

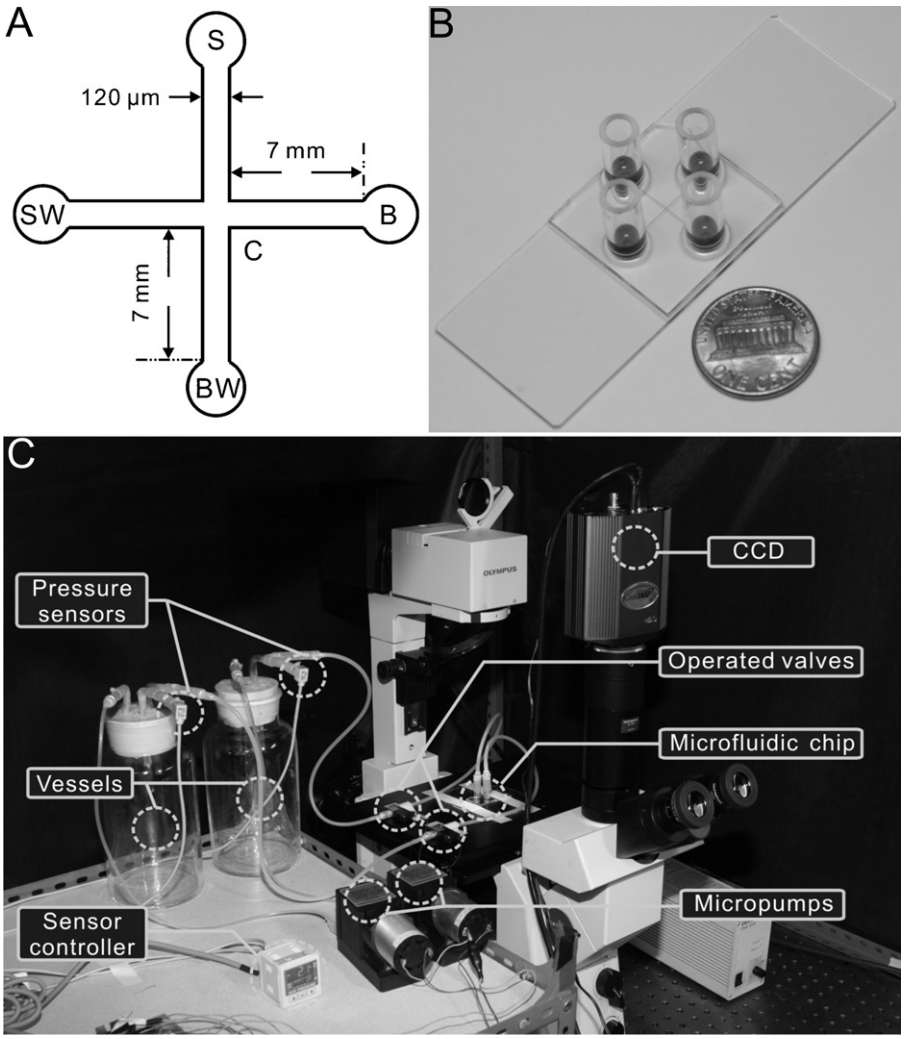

Fig. 1. (a) Chip design. (b) Picture of the chip. S for sample, SW for sample waste, B for buffer and BW for buffer waste. C indicated the intersection of the microchannel. (c) A photograph of the experimental setup.

desensitization of receptors could be minimized by shortening the durations of agonist treatment (Sabounchi et al., 2006; Savchenko et al., 1995; Sinclair et al., 2002), it is possible to realize multiple detections on a single cell by introducing millisecond samples in a pulsatile manner.

In this paper, a microfluidic cell-based biosensor (μCBB) was developed, integrating a millisecond chemical pulse generator for sample introduction and a single NIH-3T3 cell expressing endogenous P2Y receptors as the sensing element. Activation of the P2Y receptors by ATP elicits a rise in $[Ca^{2+}]_i$. After cell adhesion to the substrate in the microchannel, pulses of ATP solutions were used to simulate input signals for investigating this μCBB. Millisecond ATP pulses were generated based on hydrodynamic gated injection. Calcium fluorescence imaging was used to characterize the changes in $[Ca^{2+}]_i$ elicited by activating the P2Y receptors. Cellular responses to repetitive 100 ms pulses of 20 μM ATP at 50 s intervals maintained at a similar level, suggesting that the receptor desensitization was minimized. A possible reason could be that the 50 s interval was sufficient for the cells to recover from the desensitization induced by short durations of ATP stimulations. Thus, the developed biosensor could be repeatedly used for detecting ATP pulses every 50 s without impact on its functionality. The cellular responses were further investigated with ATP pulses of varying concentrations and durations. Results suggested a sensitivity of 2 μM for the developed μCBB. In addition, 20 μM ATP pulses with duration as short as 50 ms resulted in the same level of Ca^{2+} response induced by sustained stimulations.

2. Materials and methods

2.1. Materials

Fluorescein, adenosine 5′-triphosphate disodium salt ($ATPNa_2$), poly-L-lysine (MW: 150,000–300,000), HEPES, penicillin, streptomycin and DMSO were purchased from Sigma–Aldrich (MO, USA). Tyrode's solution as the buffer solution was prepared with 137 mM NaCl, 5.4 mM KCl, 1.3 mM $CaCl_2$, 1 mM $MgCl_2$, 10 mM glucose, and 10 mM HEPES (pH 7.2). 1 mM stock solution of Fluo-3/AM (Biotium, USA) dissolved in DMSO was diluted by buffer solutions to a final concentration of 10 μM. ATP was prepared in buffer solutions with final concentrations of 2 μM, 20 μM and 200 μM. All reagents were of analytical grade or otherwise specified. All solutions were prepared with water purified by the Millipore-Q system (Millipore, USA) and filtered with a 0.22 μm microporous membrane.

2.2. Chip design and fabrication

We designed and fabricated a cross-shaped microchannel (width, 120 μm; height, 40 μm; length of each channel, 7 mm) with

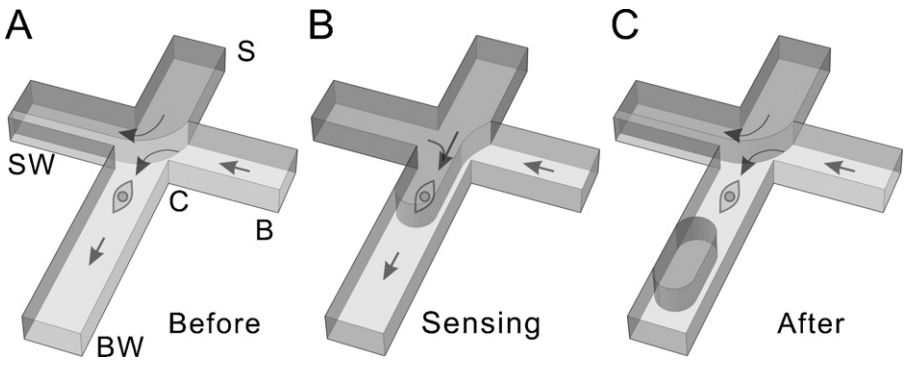

Fig. 2. Schematic of the sample introduction in the microfluidic cell-based biosensor. (a) Before sensing the chemical, hydrodynamic gating was realized by applying negative pressures to SW and BW. (b) Sensing the chemical with this cell-based biosensor by hydrodynamic gated injection for a short period of time after instant removal of the negative pressure on SW. (c) Completion of one chemical detection by reapplying the negative pressure to SW.

polydimethylsiloxane (PDMS) as the structural material (Fig. 1a and b). In brief, SU-8™ (GM1070, Gersteltec Sarl, Switzerland) mold was fabricated on a 3-in silicon wafer by rapid prototyping (Duffy et al., 1998). PDMS microchannel was formed by pouring the mixture of sylgard 184 silicone elastomer and curing agent (Dow Coming, USA) at a mass ratio of 10:1 onto the SU-8™ mold. Through-membrane holes (3 mm in diameter) were punched at each end of the microchannel after curing at 65 °C for 4 h. The PDMS layer (~1 mm thick) was then peered off from the SU-8™ mold and irreversibly bonded to a glass substrate (76 mm × 26 mm × 1.2 mm) after oxygen plasma treatment (PDC-GC-M, Weike Spectrum, Chengdu, China). Quartz tubes (inner diameter, 4 mm; height, 12 mm) were attached on the punched holes as reservoirs.

2.3. Apparatus

As illustrated in Fig. 1c, the experimental apparatus consists of a microfluidic chip, two controllable negative pressure systems and an optical detection system. To establish a negative pressure system, the negative pressure was generated in a 1 L air container by a micro-vacuum pump (Model FM2002, Ruiyi, China), and monitored by a pressure sensor (PSE541, SMC, Japan). A multichannel pressure sensor controller (PSE200, SMC, Japan) was used to regulate and stabilize the pressure with a resolution of 0.1 kPa. A three-way solenoid operated valve (Energize time, 1.4 ms; De-energize time, 2.0 ms; Series 33, MAC, USA), connecting between an air container and a reservoir via silicone tubes, was used for switching pressure upon the reservoir between negative pressure and atmospheric pressure. A LabVIEW™ (National Instruments, USA) program was written to control the solenoid valve via a PCI controller card (NI6703, National Instruments, USA), and to realize automatic chemical stimulation with varying injection times, relaxation times and number of cycles.

Experiments were carried out on an inverted microscope (IX71, Olympus, Japan) equipped with a CCD camera (CoolSNAP cf2, Photometrics) for image acquisition. The light emitted from a 100 W mercury lamp (USH1030L, Olympus), attenuated by a neutral density filter (ND-6), was filtered by a 460–490 nm band-pass filter, reflected by a 505 nm dichroic mirror, and then focused on the microchannel (a beam-spot of ~50 μm in diameter) by a 60× objective (NA 0.7). The fluorescent signal was collected through the same objective, filtered by a 510 nm high-pass filter, and finally detected by a photon counter (PMS 400A, B&H GmbH, Berlin, Germany) at 20 Hz (Fluo-3) or 2000 Hz (fluorescein) sampling rate. Temperature was maintained at 37 °C by using a heating plate (Olympus, Japan) during experiments if not emphasized.

2.4. Cell culture and maintenance

NIH-3T3 fibroblasts were maintained in Dulbecco's modified eagle medium (DMEM, Gibco) supplemented with 10% (v/v) newborn calf serum (NCS, Gibco), 100 U mL^{-1} penicillin and 100 μg mL^{-1} streptomycin at 37 °C in a humidified atmosphere of 5% CO_2. Cells were harvested after treatment with 0.2% (w/v) Trypsin-EDTA solution (Gibco) and suspended in culture media at a final concentration of ~1×10^6 cells mL^{-1}.

2.5. Cell culture on chips

Before cell seeding, PDMS microchannel was treated with oxygen plasma, and sterilized with 75% ethanol for 15 min. After the removal of ethanol, the microchannel was incubated with 0.1% (w/v) poly-L-lysine at 37 °C for 5 h and rinsed with buffer solutions, cell culture media sequentially.

Cell suspension was added to reservoir BW, and equal volumes of culture media were added to other three reservoirs. Cells were transported in channel C-BW in a pulsatile manner by applying pressure pulses to S. Cell movement for each pulse can be flexibly controlled by adjusting the pressure magnitude and duration. The minimal movement of the cells was ~100 μm, which was attained with an application of negative pressure (0.6 kPa) for 1 ms. One cell in the middle stream in the channel C-BW was selected as the target cell and finally located within 100 μm downstream the intersection of the cross-shaped microchannel (Fig. S1, Video S1). After cell seeding, the microchip was transferred to a CO_2 incubator for cell culture.

After 12-h incubation at 37 °C, cells adhered to the bottom of the microchannel. Adherent cells were then incubated with 10 μM Fluo-3/AM at 37 °C for 45 min, rinsed with buffer solutions for three times, and ready for experiments.

2.6. Experimental procedure

Sample and buffer solutions were supplied to sample reservoir (S) and buffer reservoir (B) respectively. Hydrodynamic gating was realized by applying negative pressures to buffer waste reservoir (BW) and sample waste reservoir (SW) with S and B open to atmosphere (Fig. 2a). For sensing chemical with this cell-based biosensor, a plug of sample solution was injected into channel C-BW by pressure switching on SW from negative pressure to atmosphere for a short time (Fig. 2b) and switching back to negative pressure again (Fig. 2c). By controlling the switching time, we were then able to apply millisecond sample pulses to adherent cells at arbitrary intervals. A demonstration of continuous sample plug injection

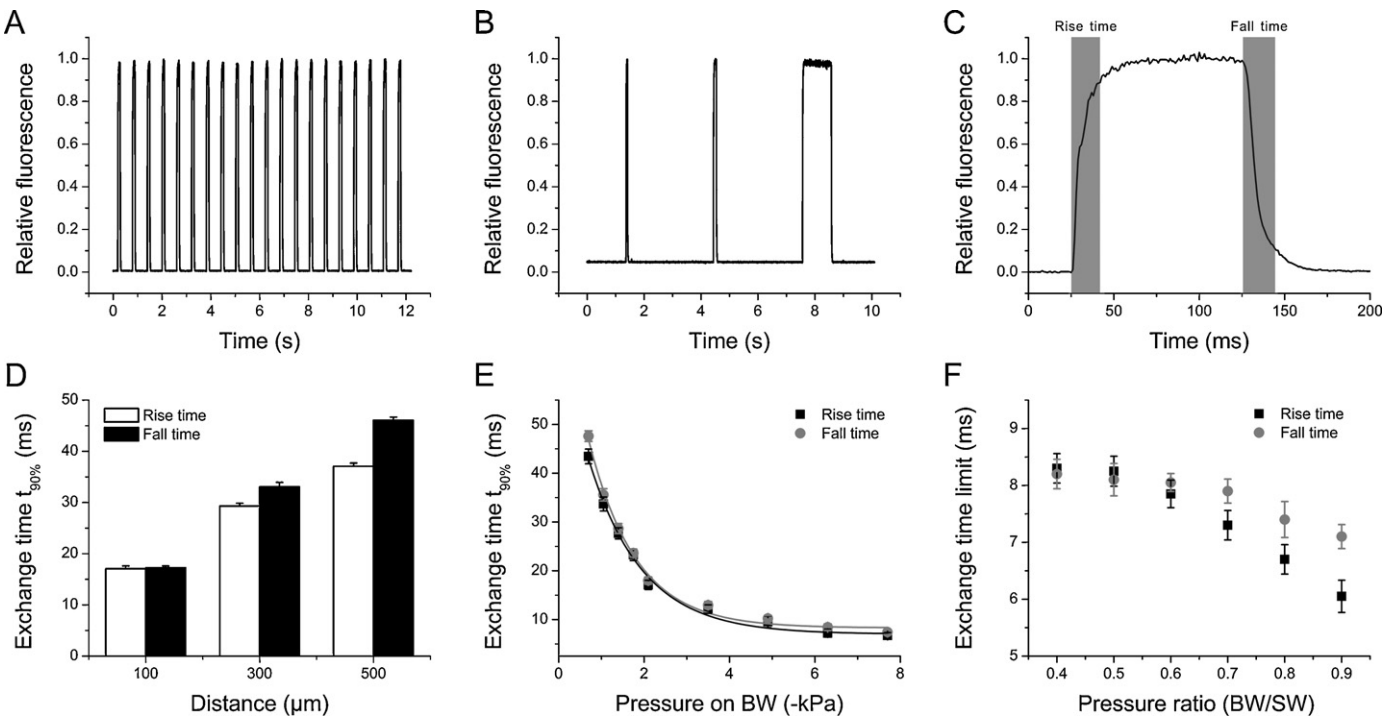

Fig. 3. Evaluation of this microfluidic chemical pulse generator. (a) Repeated injections of fluorescein for 100 ms at 500 ms intervals. (b) Injections of fluorescein for 50 ms, 100 ms and 1 s. (c) A 100 ms pulse with rise time and fall time indicated as gray areas. (d) The relationship between solution exchange time and the distance from the target cell to the intersection. (e) Pressure effect on rise time (black square) and fall time (gray circle) fitted with single exponential functions. Negative pressures on BW and SW were maintained at a ratio of 0.7. (f) Pressure ratio effect on rise time (black square) and fall time (gray circle). Negative pressure on BW was maintained at −7.7 kPa. Error bars indicate the standard deviation ($n = 10$).

with fluorescein is given in Video S2. To get more details on hydrodynamic gated injection, please see (Chen et al., 2010a, b).

2.7. Data processing

Since Fluo-3 was used as the intracellular calcium indicator, the baseline of recorded fluorescence signals (F_C) fell due to photobleaching (Thomas et al., 2000). A previous reported method was used to process the recorded fluorescence data (Feng et al., 2007). Briefly, the background (F_B) was first subtracted from the recorded fluorescence (F_C) to yield the final signal (F) (Fig. S2a). Subsequently, a mono-exponential function (F_0) was fitted to the baseline of the fluorescence signal F (Fig. S2b). The normalized fluorescence was then calculated by $(F - F_0)/F_0$ (Fig. S2c).

3. Results and discussion

The use of cell-based biosensors is usually limited by the desensitization of cell-surface receptors upon sustained exposure to sample solutions. Here, a microfluidic cell-based biosensor (μCBB) was developed, integrating a millisecond chemical pulse generator for sample introduction, which could minimize the desensitization of receptors and extend the use times. NIH-3T3 cells expressing endogenous ATP receptors were employed as the sensing element. Pulses of ATP solutions were used to simulate input signals for investigating the developed biosensor.

3.1. Characterization of endogenous ATP receptors

The developed μCBB utilized NIH-3T3 cells expressing endogenous P2Y receptors as the sensing elements. Activation of P2Y receptors by ATP elicits changes in $[Ca^{2+}]_i$. Upon binding of ATP, P2Y receptors activate phospholipase C (PLC), which catalyzes the hydrolysis of phosphatidylinositol bisphosphate (PIP_2) into inositol trisphosphate (IP_3) and diacylglycerol (DG). IP_3 binds to IP_3 receptors (IPR), leading to Ca^{2+} release from the internal Ca^{2+} stores (endoplasmic reticulum, ER) to the cytoplasm (Dubyak and el-Moatassim, 1993). The rise of intracellular calcium can then be detected using Ca^{2+} indicator. Once $[Ca^{2+}]_i$ reaches a relatively high value, Ca^{2+}-ATPase pumps Ca^{2+} back into ER, resulting in the decrease of fluorescence (Fig. S3).

The subtypes of P2Y receptors involved in ATP-induced calcium release in murine cells are $P2Y_1$, $P2Y_2$ and $P2Y_4$ receptors (Burnstock, 2004). To determine the specific receptors expressed in NIH-3T3 cells, RT-PCR analysis of the P2Y receptors mentioned above was carried out, which revealed that $P2Y_2$ receptors were abundantly expressed compared with $P2Y_1$ and $P2Y_4$ receptors (Fig. S4). In addition, $P2Y_2$ receptors have been proven to be the most sensitive receptors to ATP (EC_{50}, ~1 μM) among the three subtypes of P2Y receptors (Burnstock, 2004). Thus, the response of NIH-3T3 cells to ATP may largely depend on $P2Y_2$ receptors.

3.2. Chemical pulse generator for sample introduction

For pulsatile sample introduction, a chemical pulse generator was developed based on hydrodynamic gating. Fluorescein was used to evaluate this chemical pulse generator. 75 μL buffer solutions were added into the four reservoirs separately. Meanwhile, pressures of −3 kPa and −2.1 kPa were applied to SW and BW respectively for hydrodynamic gating. The buffer solution in S was then replaced by 1×10^{-5} M fluorescein. Repeated 100 ms injections of fluorescein at 500 ms intervals were conducted to investigate the repeatability of this method. A relative standard deviation (RSD) of the peak height was 0.2% ($n = 20$), showing an outstanding reproducibility of pulse generation (Fig. 3a). By controlling the injection time, pulses of fluorescein with variable durations (50 ms, 100 ms and 1 s) were also achieved (Fig. 3b). A typical 100 ms pulse is shown in Fig. 3c. The rise time and fall

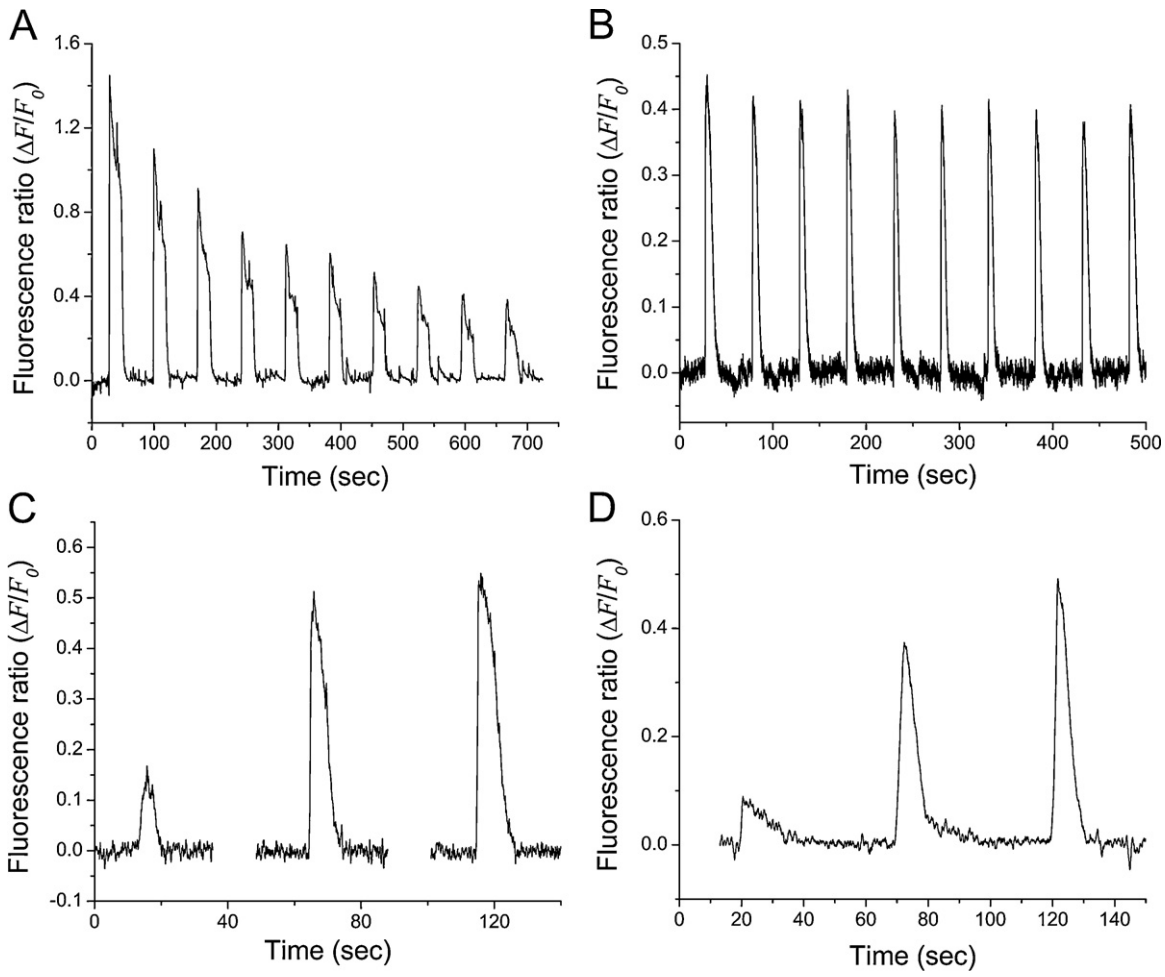

Fig. 4. Intracellular Ca^{2+} responses to repetitive 20 s pulses of 20 μM ATP (a), repetitive 100 ms pulses of 20 μM ATP (b), 100 ms pulses of 2 μM, 20 μM, 200 μM ATP (c), 2 μM ATP pulses of 30 ms, 50 ms, 100 ms (d) at 50 s intervals.

time corresponding to 90% change in fluorescence intensity was 17 ± 0.3 ms and 18 ± 0.2 ms respectively (n = 10), indicating a very fast solution exchange. The effect of detection distance on the speed of solution exchange was tested by setting detection spot at 100 μm, 300 μm and 500 μm from the intersection. As illustrated in Fig. 3d, the solution exchange time increased progressively with increasing distances, which was a major reason for the precise cell location within 100 μm downstream the intersection of the microchannel.

To further determine the solution exchange speed limit, the pressure effect on both the rise and fall time was investigated. The negative pressures on BW and SW were kept at a constant ratio of 0.7 to maintain the distribution of reagents in the microchannel. An exponential decrease was observed for both the rise and fall time with increasing negative pressures on BW (0.7, 1.1, 1.4, 1.8, 2.1, 4.9, 6.3 and 7.7 kPa), indicating a minimum solution exchange time of ~7 ms (Fig. 3e). Furthermore, the pressure on BW was kept at −7.7 kPa and the pressure ratio of BW to SW was varied. As the pressure ratio increases from 0.4 to 0.9 in 0.1 steps, the rise time and fall time slightly decreased by 1–2 ms (Fig. 3f). A possible reason could be that the solution exchange time was primarily limited by Taylor–Aris dispersion in addition to molecular diffusion and surface absorption (Bae et al., 2009; Datta and Ghosal, 2009). However, live cell experiments forced an upper limit of the flow rate. Wall shear stress (τ_w) was estimated by $\tau_w = 6\mu Q/wh^2$, where μ is the dynamic viscosity of water, w is the microchannel width and h is the microchannel height. Flow rates (Q) during injections were calculated using Hagen–Poiseuille equation. When the negative pressure on BW was above 3.5 kPa, the wall shear stress was more than 5 Pa, which might be harmful to living cells (Kuczenski et al., 2009). Thus, −2.1 kPa and −3 kPa were selected as the optimal pressures on BW and SW for the following experiments.

3.3. Detecting ATP pulses by μCBB

Since the shear stress may induce calcium transients in endothelial cells (Schwarz et al., 1992), we evaluated the effect of shear stress on $[Ca^{2+}]_i$ by exposing the cells to pulses of buffer solutions. As a result, the $[Ca^{2+}]_i$ remained constant (Fig. S5), suggesting that the abrupt change of shear stress did not account for calcium spikes during hydrodynamic gated sample injection. Meanwhile, changes in cell morphology were not observed after injections of buffer solutions for 10 min, indicating that the shear stress was not harmful to living cells. Previous literature showed that NIH-3T3 cells responded to ATP at the concentrations from 1 μM to 100 μM in a dose-dependent manner (Giovannardi et al., 1992). Thus, pulses of 20 μM ATP were used to simulate input signals for investigating the μCBB.

When 20 s pulses of 20 μM ATP were introduced with 50 s intervals, the amplitude of calcium spikes decreased gradually due to receptor desensitization (Fig. 4a). In contrast, with pulse duration of 100 ms, the amplitude of calcium spikes maintained at a similar level (Fig. 4b). The same results were observed in another 6 cells (Fig. S6), suggesting that ATP-induced desensitization of P2Y recep-

tors was minimized with ATP pulses of short durations (100 ms, 50 s intervals). The 50 s interval was sufficient for NIH-3T3 cells to recover from the desensitization induced by 100 ms ATP stimulations. Thus, the developed μCBB utilizing a single cell could be repeatedly used for the detection of the chemical with millisecond pulses of sample solutions.

To test the sensitivity of this μCBB to ATP, 100 ms pulses of ATP with increasing concentrations of 2 μM, 20 μM and 200 μM were injected for stimulations of one cell. Next, 2 μM pulses with increasing durations of 30 ms, 50 ms and 100 ms were applied to another cell. Significant increases of $[Ca^{2+}]_i$ in response to 2 μM ATP were observed (Fig. 4c and d), indicating a high sensitivity of this cell-based biosensor for detecting ATP. However, the sensitivity was related to the environmental temperature, because $[Ca^{2+}]_i$ responses to millisecond stimulus were never observed when the temperature was below 28 °C. When the temperature was set to 25 °C, with pulse durations of a few seconds, the response time of $[Ca^{2+}]_i$ were 2.15 ± 0.80 s ($n = 8$), much longer than ~500 ms response time with millisecond stimulations at 37 °C. Thus, it is necessary to integrate a miniature temperature control system for practical applications of the μCBB in the future.

To further investigate the cellular responses to ATP pulses with millisecond durations used in the μCBB and second durations used in the other CBBs, 20 μM pulses of ATP with increasing durations of 50 ms, 100 ms, 1 s and 10 s were applied to the same single cells. Fig. 5a showed a typical result that the amplitude of four Ca^{2+} spikes maintained at a similar level, which was further proved by a statistic result of experiments on 12 individual cells (Fig. 5b). It showed that millisecond pulses of 20 μM ATP resulted in the same level of Ca^{2+} response that was induced by sustained stimulations. However, the decay time, defined as a time for $[Ca^{2+}]_i$ decline, increased significantly as the duration increased from 100 ms to 1 s and 10 s. Moreover, the response time, defined as a time from ATP addition to the onset of a Ca^{2+} spike, decreased gradually (Fig. 5c).

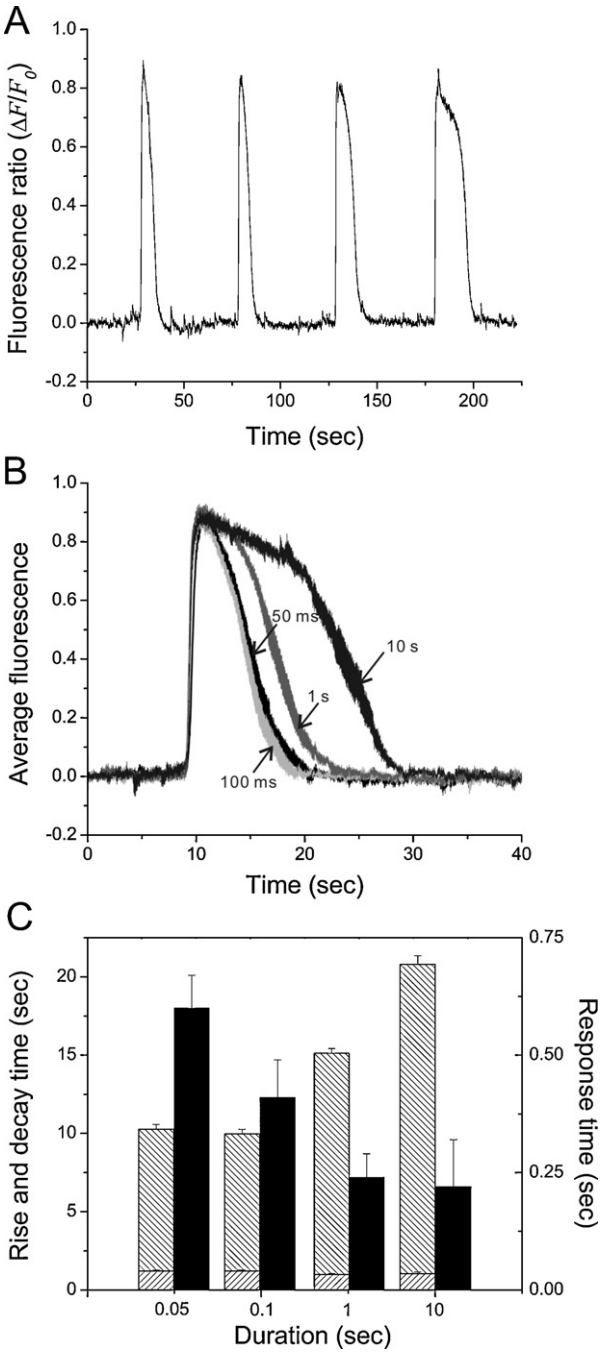

Fig. 5. (a) Intracellular Ca^{2+} responses to 20 μM ATP pulses of 50 ms, 100 ms, 1 s and 10 s. (b) Overlay of the four Ca^{2+} spikes in (a) ($n = 12$). (c) A statistic result of the response time (black), rise time (oblique) and decay time (under oblique) of the four Ca^{2+} spikes. Error bars indicate standard errors.

4. Conclusions

This paper describes a microfluidic cell-based biosensor (μCBB) for ATP detections. The μCBB integrates a millisecond chemical pulse generator for sample introduction and a single NIH-3T3 cell expressing P2Y receptors as the sensing element. Millisecond ATP pulses were generated based on hydrodynamic gated injection, which were used to simulate input signals for investigating the developed biosensor. The selective recognition of ATP by P2Y receptors elicits rises in intracellular Ca^{2+} concentrations that were monitored optically by calcium fluorescence imaging. The amplitude of the resulting calcium spikes maintained at a similar level when the cell was exposed to 100 ms pulses of 20 μM ATP at 50 s intervals, indicating that the developed μCBB could be used to detect repetitive ATP pulses every 50 s without impact on its functionality. Further investigation of the cellular responses to ATP pulses of varying concentrations and durations suggested that 20 μM ATP pulses with duration as short as 50 ms resulted in the same level of Ca^{2+} response induced by sustained stimulations.

Acknowledgements

The authors gratefully acknowledge the financial supports from National Basic Research Program of China (2007CB914203, 2007CB714507) and National Natural Science Foundation of China (30600134, 20875035 and 30800286).

Appendix A. Supplementary data

Supplementary data associated with this article can be found, in the online version, at doi:10.1016/j.bios.2011.01.013.

References

Aravanis, A.M., DeBusschere, B.D., Chruscinski, A.J., Gilchrist, K.H., Kobilka, B.K., Kovacs, G.T.A., 2001. Biosens. Bioelectron. 16, 571–577.
Bae, A.J., Beta, C., Bodenschatz, E., 2009. Lab Chip 9, 3059–3065.
Banerjee, P., Bhunia, A.K., 2009. Trends Biotechnol. 27, 179–188.
Boehm, S., Kubista, H., 2002. Pharmacol. Rev. 54, 43–99.
Burnstock, G., 2004. Curr. Top. Med. Chem. 4, 793–803.
Chen, P., Feng, X.J., Sun, J., Wang, Y., Du, W., Liu, B.F., 2010a. Lab Chip 10, 1472–1475.
Chen, P., Feng, X.J., Hu, R., Sun, J., Du, W., Liu, B.F., 2010b. Anal. Chim. Acta 663, 1–6.
Curtis, T., Naal, R.M.Z.G., Batt, C., Tabb, J., Holowka, D., 2008. Biosens. Bioelectron. 23, 1024–1031.
Datta, S., Ghosal, S., 2009. Lab Chip 9, 2537–2550.

Dubyak, G.R., el-Moatassim, C., 1993. AJP-Cell Physiol. 265, C577–606.
Duffy, D.C., McDonald, J.C., Schueller, O.J.A., Whitesides, G.M., 1998. Anal. Chem. 70, 4974–4984.
Feng, X.J., Castracane, J., Tokranova, N., Gracias, A., Lnenicka, G., Szaro, B.G., 2007. Biosens. Bioelectron. 22, 3230–3237.
Fishman, H.A., Greenwald, D.R., Zare, R.N., 1998. Annu. Rev. Bioph. Biom. 27, 165–198.
Fishman, H.A., Orwar, O., Allbritton, N.L., Modi, B.P., Shear, J.B., Scheller, R.H., Zare, R.N., 1996. Anal. Chem. 68, 1181–1186.
Giovannardi, S., Racca, C., Bertollini, L., Sturani, E., Peres, A., 1992. Cell Res. 202, 398–404.
Gray, S.A., Kusel, J.K., Shaffer, K.M., Shubin, Y.S., Stenger, D.A., Pancrazio, J.J., 2001. Biosens. Bioelectron. 16, 535–542.
Hayashi, S., Hazama, A., Dutta, A.K., Sabirov, R.Z., Okada, Y., 2004. Sci. Signal. 2004, pl14.
Hazama, A., Hayashi, S., Okada, Y., 1998. Pflügers Arch- Eur. J. Physiol. 437, 31–35.
Hu, J., 2009. Biosens. Bioelectron. 24, 1083–1089.
Klemic, K.G., Klemic, J.F., Reed, M.A., Sigworth, F.J., 2002. Biosens. Bioelectron. 17, 597–604.
Kuczenski, B., Ruder, W.C., Messner, W.C., LeDuc, P.R., 2009. PLoS One 4, e4847.
Lee, S.H., Jun, S.B., Ko, H.J., Kim, S.J., Park, T.H., 2009. Biosens. Bioelectron. 24, 2659–2664.
Matsubara, Y., Murakami, Y., Kobayashi, M., Morita, Y., Tamiya, E., 2004. Biosens. Bioelectron. 19, 741–747.
Sabounchi, P., Ionescu-Zanetti, C., Chen, R., Karandikar, M., Seo, J., Lee, L.P., 2006. Appl. Phys. Lett. 88, 183901.
Savchenko, A., Glossmann, H., Hering, S., 1995. Pflügers Arch- Eur. J. Physiol. 429, 436–442.
Schwarz, G., Callewaert, G., Droogmans, G., Nilius, B., 1992. J. Physiol. 458, 527–538.
Sigworth, F.J., Klemic, K.G., 2002. Biophys. J. 82, 2831–2832.
Sinclair, J., Pihl, J., Olofsson, J., Karlsson, M., Jardemark, K., Chiu, D.T., Orwar, O., 2002. Anal. Chem. 74, 6133–6138.
Suska, A., Ibanez, A.B., Lundstrom, I., Berghard, A., 2009. Biosens. Bioelectron. 25, 715–720.
Thomas, D., Tovey, S.C., Collins, T.J., Bootman, M.D., Berridge, M.J., Lipp, P., 2000. Cell Calcium 28, 213–223.
Xu, G.X., Ye, X.S., Qin, L.F., Xu, Y., Li, Y., Li, R., Wang, P., 2005. Biosens. Bioelectron. 20, 1757–1763.
Zhang, X.L., Yin, H.B., Cooper, J.M., Haswell, S.J., 2006. Electrophoresis 27, 5093–5100.